

NUMERICAL INVESTIGATION ON CONVECTIVE HEAT TRANSFER ENHANCEMENT USING VARIOUS NANO FLUIDS AND DIFFERENT DUCT GEOMETRIES



Name of Candidates

SAI PRANEETH JANGAM(711956)

KADIYAM SRIKAR(711928)

D SAI GANESH(711919)

VADDI YUVARAJ(711961)

DEPARTMENT OF MECHANICAL ENGINEERING

NATIONAL INSTITUTE OF TECHNOLOGY

ANDHRA PRADESH -534102, INDIA.

**NUMERICAL INVESTIGATION ON CONVECTIVE HEAT TRANSFER
ENHANCEMENT USING VARIOUS NANO FLUIDS AND DIFFERENT DUCT
GEOMETRIES**

*Thesis submitted to
National Institute of Technology Andhra Pradesh
for the award of the degree of Bachelor of Technology by*

SAI PRANEETH JANGAM (Enrolment No: 711956)

KADIYAM SRIKAR (Enrolment No: 711928)

D SAI GANESH (Enrolment No: 711919)

VADDI YUVARAJ (Enrolment No: 711961)

Supervisor
Dr.G.Santhosh kumar
Dept. of Mechanical Engineering



**DEPARTMENT OF MECHANICAL ENGINEERING
NATIONAL INSTITUTE OF TECHNOLOGY,
ANDHRA PRADESH -534102, INDIA**

APPROVAL SHEET

This thesis/dissertation/report entitled **NUMERICAL INVESTIGATION ON CONVECTIVE HEAT TRANSFER ENHANCEMENT USING VARIOUS NANO FLUIDS AND DIFFERENT DUCT GEOMETRIES** by Sai Praneeth Jangam, Kadiyam Srikanth, D.Sai Ganesh, Vaddi Yuvaraj is approved for the degree of ‘Bachelor of Technology’.

Supervisor (s)

Examiners

Chairman

Date :

Place :

DECLARATION

I declare that this written submission represents my ideas in my own words and where others' ideas or words have been included, I have adequately cited and referenced the original sources. I also declare that I have adhered to all principles of academic honesty and integrity and have not misrepresented or fabricated or falsified any idea/data/fact/source in my submission. I understand that any violation of the above will be cause for disciplinary action by the Institute and can also evoke penal action from the sources which have thus not been properly cited or from whom proper permission has not been taken when needed.

(Signature)

Sai Praneeth Jangam

(711956)

Date:

DECLARATION

I declare that this written submission represents my ideas in my own words and where others' ideas or words have been included, I have adequately cited and referenced the original sources. I also declare that I have adhered to all principles of academic honesty and integrity and have not misrepresented or fabricated or falsified any idea/data/fact/source in my submission. I understand that any violation of the above will be cause for disciplinary action by the Institute and can also evoke penal action from the sources which have thus not been properly cited or from whom proper permission has not been taken when needed.

(Signature)

Kadiyam Srikar

(711928)

Date:

DECLARATION

I declare that this written submission represents my ideas in my own words and where others' ideas or words have been included, I have adequately cited and referenced the original sources. I also declare that I have adhered to all principles of academic honesty and integrity and have not misrepresented or fabricated or falsified any idea/data/fact/source in my submission. I understand that any violation of the above will be cause for disciplinary action by the Institute and can also evoke penal action from the sources which have thus not been properly cited or from whom proper permission has not been taken when needed.

(Signature)

D Sai Ganesh

(711919)

Date:

DECLARATION

I declare that this written submission represents my ideas in my own words and where others' ideas or words have been included, I have adequately cited and referenced the original sources. I also declare that I have adhered to all principles of academic honesty and integrity and have not misrepresented or fabricated or falsified any idea/data/fact/source in my submission. I understand that any violation of the above will be cause for disciplinary action by the Institute and can also evoke penal action from the sources which have thus not been properly cited or from whom proper permission has not been taken when needed.

(Signature)

Vaddi Yuvaraj

(711961)

Date:

CERTIFICATE

It is certified that the work contained in the thesis titled "**NUMERICAL INVESTIGATION ON CONVECTIVE HEAT TRANSFER ENHANCEMENT USING VARIOUS NANO FLUIDS AND DIFFERENT DUCT GEOMETRIES**" by "Sai Praneeth Jangam, bearing Roll No: 711956", "Kadiyam Srikanth, bearing Roll No: 711928", "D Sai Ganesh, bearing Roll No: 711919", "Vaddi Yuvaraj, bearing Roll No: 711961" has been carried out under my/our supervision and that this work has not been submitted elsewhere for a degree*

Signature of Supervisor(s)

Dr. G. SANTOSH KUMAR

Assistant Professor

Mechanical Department

N.I.T. Andhra Pradesh

November,2022

ACKNOWLEDGEMENT

We would like to give our deepest and sincere appreciation and gratitude to **Dr.G.Santhosh kumar**, for his invaluable guidance, constructive criticism, and encouragement during this project.

We also extend our thanks to the entire **Department of Mechanical Engineering** for giving us this opportunity to accomplish this project. Last but not the least, we express our profound gratitude to the Almighty and our parents for their blessings and support without which this task could have never been accomplished.

LIST OF FIGURES

LIST OF TABLES

Table. No	Name	Page.no
1	Material Properties.	8
2,3,4	Thermophysical properties of TiO ₂ , Al ₂ O ₃ and SiO ₂	8 ,9
5	Grid Independence analysis	12

ABSTRACT

This project report explores the potential of using nanofluids to enhance the performance of a solar water heater. The study investigates the convective heat transfer performance of three types of nanofluids, SiO₂, TiO₂, and Al₂O₃, at different volume concentrations and Richardson numbers. Computational fluid dynamics software ANSYS Fluent 18.1 is used to simulate the heat transfer performance in an equilateral triangular cross sectioned duct and six other geometries. A mesh sensitivity test is conducted to optimize the mesh size for the simulation

The results indicate that Al₂O₃ nanofluid exhibits the highest heat transfer enhancement among the three types of nanofluids. Furthermore, the optimal concentration of nanoparticles for the highest heat transfer performance varies with the geometry of the duct and the Richardson number. These findings have significant implications for the design and optimization of solar water heaters using nanofluids and could contribute to the development of more efficient and sustainable solar energy systems.

CONTENTS

Title Page	i
Certificate of Approval	iii
Declaration	iv
Certificate	viii
Acknowledgement	ix
List of Figures	x
List of Tables	xi
Abstract	xii
Contents	xii i
Chapter 1 Introduction	1
1.1 Problem of Using Fossil fuels and alternatives	1
1.2 How does Solar Heater work?	2
1.3 Why are we using various Nanofluids and different geometries	2
Chapter 2 Literature Review	3
Chapter 3 Problem Formulation	6
Chapter 4 Methodology	7
4.1 Methodology Overview	7
4.1.1 Geometrical description	8
4.1.2 Boundary Conditions	8
4.1.3 Numerical Methodology & Techniques	9
4.1.4 Material Properties & Thermo-Physical properties of the fluids	11
4.1.5 Meshing	12
4.1.6 Grid Independent Analysis	12
4.1.7 Validation	14

Chapter 5 Results and Discussion	16
5.1 Convective Heat Transfer Performance for Al ₂ O ₃ -water	16
based nanofluids for different Richardson numbers & volume concentration values	
5.1.1 Heat Transfer Coefficients	16
5.1.2 Nusselt Numbers	17
5.1.3 Average Shear stresses	18
5.1.4 Heat Transfer Coefficient in wall-2 & wall-3	19
5.1.5 Pumping Power	20
5.2 Convective Heat Transfer Performance for TiO ₂ -water	
based nanofluids for different Richardson numbers & volume concentration values	21
5.2.1 Heat Transfer Coefficients	21
5.2.2 Nusselt Numbers	22
5.2.3 Average Shear stresses	23
5.2.4 Heat Transfer Coefficient in wall-2 & wall-3	24
5.2.5 Pumping Power	25
5.3 Convective Heat Transfer Performance for SiO ₂ -water	
based nanofluids for different Richardson numbers & volume concentration values	26
5.3.1 Heat Transfer Coefficients	26
5.3.2 Nusselt Numbers	27
5.3.3 Average Shear stresses	28
5.3.4 Heat Transfer Coefficient in wall-2 & wall-3	29
5.3.5 Pumping Power	30

5.4 Comparing Convective heat transfer performance between nanofluids using analytical data	31
5.4.1 Comparing HTC	31
5.4.2 Comparing Nusselt Number	32
5.4.3 Comparing Average Shear Stress	33
5.4.4 Comparing Results between Pumping Power	35
5.5 Observing Convective heat transfer performance between Nanofluids using streamline contours	36
5.5.1 Contours of Aluminium Oxide NanoFluid	36
5.5.2 Contours of Titanium Oxide NanoFluid	38
5.5.3 Contours of Silicon Oxide NanoFluid	40
Chapter 6 Conclusion	
Chapter 7 Future scope of work	
Nomenclature	
References	

Chapter 1

Introduction

Fossil fuels such as coal, oil, and gas have been the primary source of energy for many years. However, the burning of fossil fuels has negative impacts on the environment and contributes to climate change. Therefore, it is important to reduce our reliance on fossil fuels and transition towards cleaner, renewable sources of energy.

One way to do this is to replace the use of fossil fuels for heating with solar heaters. Solar heaters use energy from the sun to heat water, which can then be used for various purposes, including space heating and domestic hot water.

The advantages of using solar heaters instead of fossil fuels include:

- Reduced greenhouse gas emissions: Solar heaters produce zero emissions, whereas the burning of fossil fuels releases carbon dioxide and other harmful gases into the atmosphere.
- Reduced dependence on non-renewable resources: Fossil fuels are finite resources, and their availability is decreasing. Solar heaters, on the other hand, rely on an abundant and renewable energy source – the sun.
- Cost savings: Although the initial cost of installing a solar heating system may be higher than that of a fossil fuel-based system, the ongoing operational costs of a solar system are much lower, as there are no fuel costs.
- Increased energy security: By using a renewable energy source such as the sun, we can reduce our reliance on fossil fuels and increase our energy security.

In summary, the use of fossil fuels has negative impacts on the environment and contributes to climate change. By replacing them with solar heaters, we can reduce greenhouse gas emissions, reduce our dependence on non-renewable resources, save costs, and increase energy security.

1.2 How does a Solar Water heater work?

A solar water heater is a device that uses energy from the sun to heat water. The basic working principle of a solar water heater involves the conversion of solar energy into heat energy, which is then used to heat the water.

The most common type of solar water heater is the flat-plate collector system. This system consists of a flat-plate collector, a storage tank, and a circulation pump. The flat-plate collector is typically made of metal or plastic and is coated with a dark, heat-absorbing material. The collector is placed on the roof of a building or in an area that receives direct sunlight.

The collector absorbs solar radiation and converts it into heat, which is then transferred to a fluid circulating through the collector. The heated fluid is then pumped through a heat exchanger that transfers the heat to the water in the storage tank. The heated water is then available for use.

1.3 Why are nanofluids in solar water heaters required?

In recent years, researchers have been exploring the use of nanofluids in solar water heaters to improve their efficiency. Nanofluids are liquids that contain small particles, typically between 1 and 100 nanometers in size. These particles can be made of metals, ceramics, or other materials and have unique properties that can improve heat transfer.

When nanofluids are used in a solar water heater, the particles in the fluid can absorb more heat from the sun than the fluid alone. Additionally, the use of nanofluids can reduce the size of the collector needed to heat the same amount of water, making the system more compact and easier to install.

In summary, a solar water heater uses energy from the sun to heat water. The basic working principle involves the conversion of solar energy into heat energy, which is then transferred to a fluid circulating through a collector and then to the water in a storage tank. The use of nanofluids in solar water heaters can improve their efficiency by allowing for more heat to be absorbed and transferred to the water.

Chapter 2

Literature Review

The use of nanofluids for convective heat transfer enhancement has been a subject of extensive research in recent years. A literature review reveals that nanofluids have the potential to significantly enhance heat transfer in various heat transfer applications.

- 1.Circular tube with CuO/water nanofluid: Both theoretical and experimental results indicate that heat-transfer coefficients increase with nanoparticle concentration as well as the Peclet number. (Ferrouillat et al., 2011)
- 2.Equilateral triangular duct with Au and SiO₂/water nanofluids: SiO₂ nanofluid has the highest Nusselt number while Au nanofluid has the lowest Nusselt number. The apex angle of the triangular duct has a remarkable influence on the Nusselt number. (Mohammed et al., 2011)
- 3.Iisosceles triangular cross-section with water: Predicted the simultaneous existence of macroscopically large stable regions of laminar and turbulent flow during the transition phenomenon. (Hanks and Cope, 1970)
- 4.Equilateral and right isosceles triangles with CuO/water nanofluid: Application of solving an integro-differential eigenvalue problem arising in the discussion of laminar flow development in ducts. (Aggarwala and Gangal, 1975)
- 5.Vertical triangular cross-section with air: Axial (perimeter averaged) heat transfer coefficients along the side of each duct are obtained for laminar and transition to turbulent regimes of natural convection heat transfer. (Ali and Al-Ansary, 2009)
- 6.Circular tube with Transformer oil + Cu nanoparticles suspension and water + Cu nanoparticles: Hot-wire method used to measure the thermal conductivity of nanofluids, with the main objective of comparing data obtained by different organizations for the same samples. (Xuan and Li, 2000)
- 7.Vertical triangular cross-section with Al₂O₃/water nanofluid: Correlations for effective thermal conductivity and viscosity are synthesized and developed based on the reported experimental data. (Khanafer and Vafai, 2011)
- 8.Circular tube with Al₂O₃/water nanofluid: Presented an experimental investigation of the specific heat of the water-based Al₂O₃ nanofluid with DSC measurement. (Zhou and Ni, 2008)

- 9.Circular tube with CuO/water nanofluid: Both theoretical and experimental results indicate that heat-transfer coefficients increase with nanoparticle concentration as well as the Peclet number. (Heris et al., 2006 and Edalati et al., 2012)
- 10.Equilateral triangular duct with Al₂O₃/water nanofluid: There is an increase in the average convective heat transfer coefficient and Nusselt number for increasing values of Richardson number and particle concentration. (Manca et al., 2012 and Heris et al., 2014)
- 11.Inclined copper tube with Al₂O₃/water nanofluid: Developed correlations to calculate the Nusselt number in the fully developed region for horizontal and vertical tubes. A higher particle volume concentration induces a decrease of the Nusselt number for the horizontal inclination. (Mansour et al., 2011)
- 12.Lee et al. (1999) investigated the use of copper nanoparticles suspended in water as a heat transfer fluid. They found that the heat transfer coefficient was significantly higher for the nanofluid than for pure water, and that the enhancement increased with increasing particle concentration and flow rate.
- 13.Das et al. (2003) studied the convective heat transfer of Al₂O₃-water and Cu-water nanofluids in a horizontal tube. They found that the heat transfer coefficient was enhanced by up to 55% for the Al₂O₃-water nanofluid and up to 95% for the Cu-water nanofluid, compared to pure water.
- 14.Wang et al. (2007) investigated the convective heat transfer of Al₂O₃-water and SiO₂-water nanofluids in a tube under laminar flow conditions. They found that the heat transfer enhancement increased with increasing nanoparticle concentration and decreasing particle size.
- 15.Kumar et al. (2015) reviewed the literature on the use of nanofluids for convective heat transfer enhancement and found that the heat transfer coefficient could be enhanced by up to 60% for certain nanofluids, compared to pure fluids. They also found that the enhancement was influenced by factors such as nanoparticle size, concentration, and shape.
- 16.Peng et al. (2017) investigated the convective heat transfer of Al₂O₃-water nanofluids in a flat plate solar collector. They found that the heat transfer coefficient was enhanced by up to 28% for the nanofluid compared to pure water, and that the enhancement increased with increasing nanoparticle concentration.

The following are some key findings from the literature review:

1. Increased thermal conductivity: Nanoparticles have much higher thermal conductivity than conventional fluids, which can significantly increase the overall thermal conductivity of the nanofluid. This enhanced thermal conductivity can improve convective heat transfer in various applications, such as heat exchangers and cooling systems.
2. Enhanced heat transfer coefficient: The presence of nanoparticles in a fluid can disrupt the fluid flow, which can lead to increased heat transfer coefficients. Studies have shown that the heat transfer coefficient of a nanofluid can be significantly higher than that of a conventional fluid.
3. Particle agglomeration: One challenge associated with the use of nanofluids is the tendency of nanoparticles to agglomerate, which can reduce their effectiveness in enhancing convective heat transfer. Researchers have investigated various methods to prevent particle agglomeration, such as using surfactants and magnetic fields.
4. Nanoparticle type and concentration: The type and concentration of nanoparticles can have a significant impact on the convective heat transfer enhancement of a nanofluid. Studies have shown that the type of nanoparticle and its concentration can affect the thermal conductivity and heat transfer coefficient of the nanofluid.
5. Applications: Nanofluids have been tested for various applications, such as heat exchangers, cooling systems, and solar collectors. The results have shown that nanofluids can significantly improve the heat transfer efficiency of these systems.

Overall, these studies demonstrate that the use of nanofluids can significantly enhance convective heat transfer, and that the extent of enhancement is influenced by various factors such as nanoparticle concentration, size, and shape. However, further research is needed to fully understand the mechanisms behind this enhancement and to optimize the use of nanofluids for heat transfer applications.

Chapter 3

Problem Formulation

Objective: To compare the convective heat transfer performance of different nanofluids (SiO_2 , TiO_2 , and Al_2O_3) at varying volume concentrations (0% - 4%) and Richardson's numbers (0.1, 0.5, 1, 2, 3, 5).

Geometry: An equilateral triangular duct with a side length of 17mm and a duct length of 2 meters is used.

Heat Flux: A uniform heat flux is applied to all three rectangular sides of the triangular cross-sectioned duct.

Additional Geometries: The study also considers six other geometries, including one rectangular duct and four isosceles trapezoidal ducts with base angles of 50, 60, 70, and 80 degrees, as well as an isosceles triangle of 45 degrees.

Nanoparticles: The nanofluids used in the study contain metallic nanoparticles such as copper, silver, and aluminium oxide.

Parameters: The study varies the volume concentration of nanoparticles in the nanofluids and the Richardson's numbers to analyse their effects on convective heat transfer.

Analysis: The convective heat transfer performance of the nanofluids is analysed using numerical simulations and compared to the performance of traditional fluids.

Chapter 4

Methodology

4.1 Steps involved process

The following is an improved methodology for studying convective heat transfer enhancement using nanofluids:

1. Experimental Setup: A steady-state and fully developed regime flow is considered for the analysis. The experiment is performed in a three-dimensional equilateral triangular duct with a side length of 17mm and a duct length of 2 meters. A uniform heat flux is applied to all three rectangular sides of the triangular cross-sectioned duct. The experiment is carried out at varying volume concentrations of SiO₂, TiO₂, and Al₂O₃ nanoparticles in water-based nanofluids.
2. Numerical Analysis: Computational fluid dynamic (CFD) code “Ansys Fluent 18.1” is used to simulate the flow and analyse the convective heat transfer enhancement. The flow is assumed to be steady-state, incompressible, and laminar, with constant temperature, and Boussinesq approximation is employed. The single-phase model approach is employed for the nanofluids, and a second-order upward scheme is employed for energy and momentum equations.
3. Validation: The numerical simulation results are validated by comparing them with existing experimental data and theoretical results from the literature. The validation is performed for the traditional fluid and nanofluid cases to ensure the accuracy of the simulation results.
4. Analysis: The convective heat transfer enhancement performance of the nanofluids is analysed by comparing the average Nusselt number and friction factor with those of the traditional fluid. The effects of varying volume concentrations, Richardson numbers, and different nanoparticle types on convective heat transfer enhancement are investigated. The results are compared to determine the optimal volume concentration and Richardson number for maximum heat transfer performance.
5. Conclusion: The study aims to provide insights into the convective heat transfer enhancement using nanofluids and determine the optimal nanoparticle concentration and geometry for maximum heat transfer performance. The results of the study can be used in

various industrial applications, including solar collectors, heat exchangers, and cooling systems

4.1.1 Geometrical description:

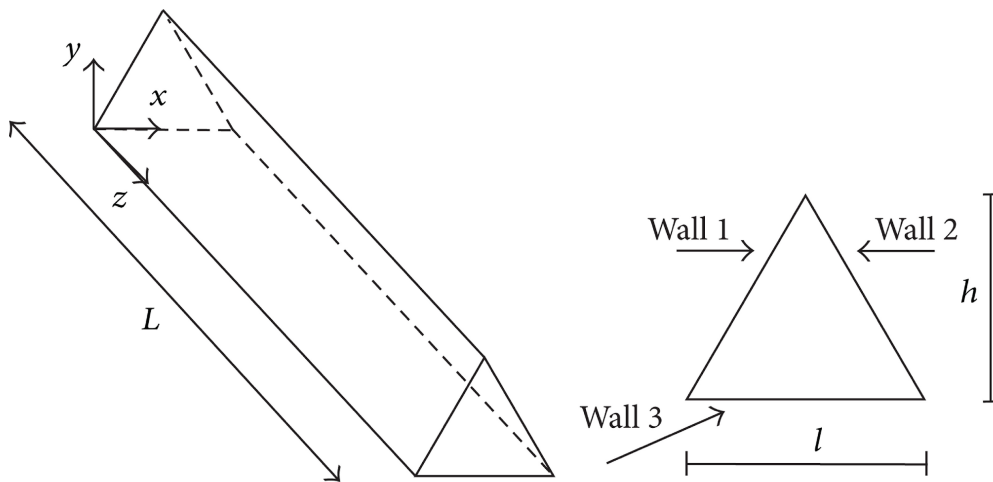


Figure-1: Equilateral triangular duct and its cross-sectional view

A three-dimensional duct with an equilateral triangular cross section is investigated as shown in figure-1. According to figure-1, the overall length L is 2.0 m, whereas the internal edge l is 0.017 m. The hydraulic diameter, $dh = 4A/Ph$, is therefore equal to 0.01 m.

4.1.2 Boundary Conditions:

The assigned boundary conditions for the study are as follows:

1. Inlet Section: The inlet section is assigned a uniform velocity and temperature profile to maintain a steady flow throughout the duct. The velocity profile is set to a constant value, and the temperature profile is also set to a constant value to ensure that the flow remains isothermal.
2. Outlet Section: The outlet section is assigned an outflow condition where the velocity components and temperature derivatives are equal to zero. This condition ensures that the fluid exits the duct without any disturbance and that the flow remains steady-state.
3. Duct Surfaces: The duct surfaces are assigned a no-slip condition, where the velocity components are equal to zero. This condition ensures that the fluid sticks to the surface of the duct and doesn't slip past it. The duct surfaces are also assigned a uniform heat flux to

maintain a constant temperature throughout the duct. This condition ensures that there is a continuous transfer of heat between the fluid and the duct surfaces.

4. Boussinesq Approximation: The Boussinesq approximation is employed to account for the buoyancy effects of the heated fluid. This approximation assumes that the fluid's density is constant except for a temperature-dependent term that is small compared to the density.

5. These boundary conditions ensure that the flow remains steady-state, isothermal, and that there is a continuous transfer of heat between the fluid and the duct surfaces. The Boussinesq approximation ensures that the buoyancy effects are taken into account, which is important for accurately analysing the convective heat transfer performance of the nanofluids

4.1.3 Numerical Methodology & Techniques:

In our study, we used ANSYS Fluent 18.1 software to create the mesh and solve the simulation in FEA. Meshing is a critical step in finite element analysis (FEA) as it determines the accuracy and reliability of the simulation results. A mesh is created by dividing the geometry into a discrete number of elements, which contain nodes that represent the shape of the object. This discretization process makes it possible to solve the problem numerically.

Continuity Equation

$$\frac{\partial u}{\partial x} + \frac{\partial v}{\partial y} + \frac{\partial w}{\partial z} = 0$$

Momentum Equations in x y z directions

$$u \frac{\partial u}{\partial x} + v \frac{\partial u}{\partial y} + w \frac{\partial u}{\partial z} + \frac{1}{\rho} \frac{\partial P}{\partial x} = \left(\frac{\partial^2 u}{\partial x^2} + \frac{\partial^2 u}{\partial y^2} + \frac{\partial^2 u}{\partial z^2} \right)$$

$$u \frac{\partial v}{\partial x} + v \frac{\partial v}{\partial y} + w \frac{\partial v}{\partial z} + \frac{1}{\rho} \frac{\partial P}{\partial y} = \left(\frac{\partial^2 v}{\partial x^2} + \frac{\partial^2 v}{\partial y^2} + \frac{\partial^2 v}{\partial z^2} \right)$$

$$u \frac{\partial w}{\partial x} + v \frac{\partial w}{\partial y} + w \frac{\partial w}{\partial z} + \frac{1}{\rho} \frac{\partial P}{\partial z} = \left(\frac{\partial^2 w}{\partial x^2} + \frac{\partial^2 w}{\partial y^2} + \frac{\partial^2 w}{\partial z^2} \right)$$

Energy Equation

$$u \frac{\partial T}{\partial x} + v \frac{\partial T}{\partial y} + w \frac{\partial T}{\partial z} = \alpha \left(\frac{\partial^2 T}{\partial x^2} + \frac{\partial^2 T}{\partial y^2} + \frac{\partial^2 T}{\partial z^2} \right)$$

Data reduction Techniques:

- The dimensionless parameters of Reynolds number, Grashof number, Richardson number, Nusselt number and friction factor are considered for the data reduction and they are expressed by the following relations:

$$Re = \frac{Vd_h}{\nu}$$

$$Gr = \frac{g \beta q (d_h)^4}{\lambda v^2}$$

$$Ri = \frac{Gr}{Re^2}$$

$$Nu_{av} = \frac{qd_h}{T_w - T_m}$$

$$f = 2 \Delta P \frac{d_h}{L} \frac{1}{\rho V^2}$$

Where V is average inlet velocity, q is heat flux, Tw and Tm represents the average surface temperature and bulk fluid temperature, respectively

Correlations formulas varying by volumetric concentrations:

Density : $\rho_{nf} = (1 - \phi)\rho_{bf} + \phi\rho_p$

Specific Heat : $(\rho c_p)_{nf} = (1 - \phi)(\rho c_p)_{bf} + \phi(\rho c_p)_p$

Thermal expansion coefficient: $\frac{\beta_{nf}}{\beta_{bf}} = \frac{1}{((1-\phi)/\phi)(\rho_{bf}/\rho_p)} \frac{\beta_p}{\beta_{bf}} + \frac{1}{((\phi/(1-\phi))(\rho_{bf}/\rho_p) + 1)}$

Dynamic viscosity : $\frac{\mu_{nf}}{\mu_{bf}} = \frac{1}{1 - 34.87(d_p/d_f)^{-0.3} \phi^{1.03}}$

$d_f = 0.1(6M/N\pi\rho_{nf,0})$ in which M is the molecular weight of the base fluid, N is the Avogadro number, and $\rho_{f,0}$ is the mass density of the base fluid calculated at $T = 293$ K

Thermal conductivity : $\frac{\lambda_{nf}}{\lambda_{bf}} = 1 + 4.4 Re^{0.4} Pr^{0.66} \left(\frac{T}{T_{fr}} \right)^{10} \cdot \left(\frac{\lambda_{nf}}{\lambda_{bf}} \right)^{0.03} \cdot \phi^{0.66}$

4.1.4 Material Properties & Thermo-Physical properties of the fluids:

Material	Density [kg/m3]	Specific Heat [J/Kg.K]	Volumetric Expansion Coefficient [1/K]	Dynamic Viscosity [Pa.s]	Thermal conductivity [W/m.K]
Water	998.2	4182	2.10E-04	9.93E-04	0.597
Al ₂ O ₃	3880	773	//	//	36
TiO ₂	4250	686.2	2.60E-08	//	8.9
SiO ₂	2220	745	4.00E-06	//	10.4

Table 1. Material Properties

Volume concentration	Density [kg/m3]	Specific Heat [J/Kg.K]	Volumetric Expansion Coefficient [1/K]	Dynamic Viscosity [Pa.s]	Thermal conductivity [W/m.K]
0%	998.2	4182	2.10E-04	9.93E-04	0.597
1%	1030.72	4037.8563	2.10E-04	1.04E-03	0.59847
2%	1063.24	3902.5296	2.09E-04	1.08E-03	0.59932
4%	1128.27	3655.2772	2.08E-04	1.20E-03	0.60067

Table 2. Water based Titanium oxide Nanofluid Thermo-physical properties at T=293 K.

Volume concentration	Density [kg/m3]	Specific Heat [J/Kg.K]	Volumetric Expansion Coefficient [1/K]	Dynamic Viscosity [Pa.s]	Thermal conductivity [W/m.K]
0%	998.2	4182	2.10E-04	9.93E-04	0.597
1%	1027	4053	2.10E-04	1.08E-03	0.622
2%	1056	3931	2.10E-04	1.19E-03	0.636
4%	1113	3707	2.09E-04	1.51E-03	0.658

Table 3. Water based Aluminum oxide Nanofluid Thermo-physical properties at T=293 K.

Volume concentration	Density [kg/m3]	Specific Heat [J/Kg.K]	Volumetric Expansion Coefficient [1/K]	Dynamic Viscosity [Pa.s]	Thermal conductivity [W/m.K]
0%	998.2	4182	2.10E-04	9.93E-04	0.597
1%	1010.42	4106.4853	2.09E-04	1.02E-03	0.600717
2%	1022.64	4032.7751	2.08E-04	1.05E-03	0.60287
4%	1047.07	3890.5152	2.07E-04	1.10E-03	0.60628

Table 4. Water based Silicon oxide Nanofluid Thermo-physical properties at T=293 K

4.1.5 Meshing:

Meshing is one of the most important steps in performing an accurate simulation using FEA. A mesh is made up of elements which contain nodes (coordinate locations in space that can vary by element type) that represent the shape of the geometry. Any continuous object has infinite degrees of freedom (DOF) which makes it impossible to solve using hand calculations. So in FEM, we create a mesh which splits the domain into a discrete number of elements for which the solution can be calculated.

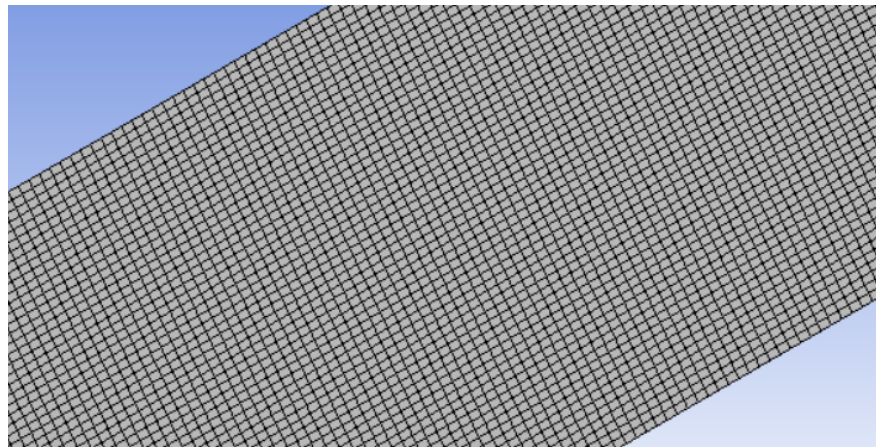


Fig-2: Meshed Triangular duct

4.1.6 Grid Independent Analysis:

In our study, we conducted a grid independence test to determine the optimal mesh size for the simulation. This test involved evaluating various grid conditions to find the smallest number

of elements without generating a difference in the numerical results. We used ANSYS Fluent 18.1 software to create the mesh and solve the simulation.

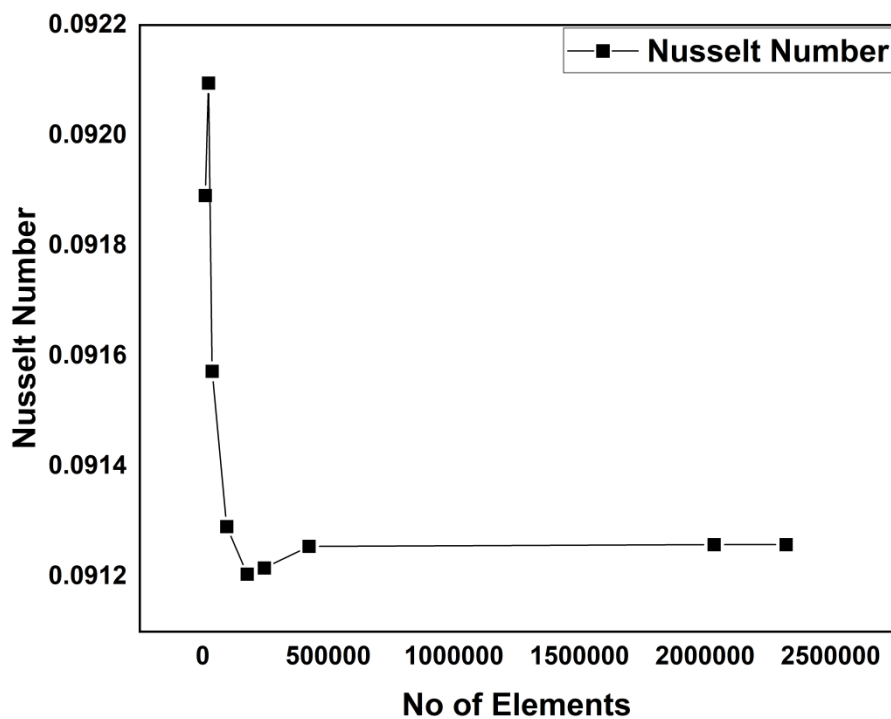
To perform the grid-sensitivity test, we used different numbers of nodes and elements for each geometry. Specifically, we used 31840, 60000, 111300, 341829, 757614, 1024458, 2296574 nodes for 22260, 44955, 87384, 287712, 662000, 903279, and 2088000 number of elements, respectively. We evaluated the Nusselt numbers for each grid size and recorded the results in Table-1.

After conducting the grid-sensitivity test, we determined that the optimal mesh size for the simulation was 0.45 mm. We used 1521856 elements and 1716900 nodes to achieve this mesh size. This mesh size allowed us to obtain accurate and reliable results while keeping the computational cost within reasonable limits.

In summary, meshing is a critical step in FEA, and the grid-sensitivity test is an essential process to determine the optimal mesh size. We determined that the optimal mesh size for our simulation was 0.45 mm.

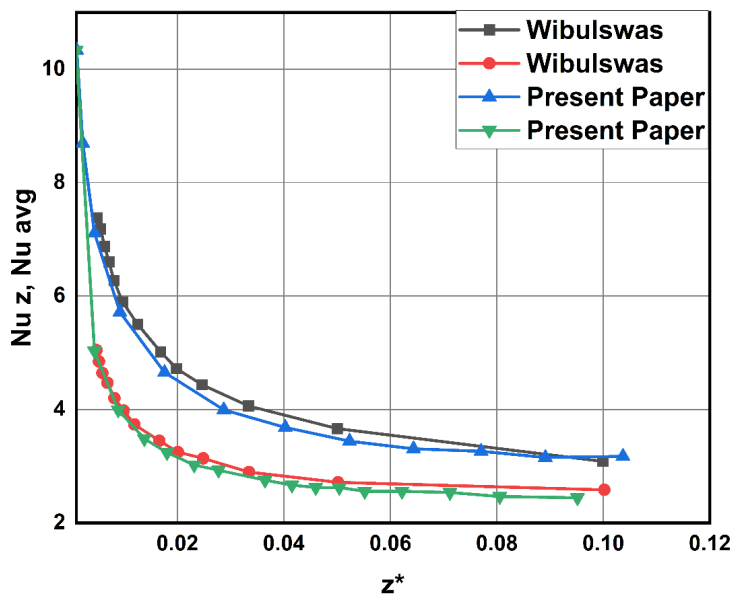
S.NO	Number of Element	Nusselt Number
1	10697	0.091891039
2	23744	0.09209474
3	37925	0.091572295
4	95944	0.091290553
5	177413	0.091204188
6	245735	0.091215578
7	424072	0.09125459
8	2036320	0.091257739
9	2323456	0.091257801

Table 5 Grid Independence Analysis



Graph 1: Grid Independent Analysis

4.1.7 Validation:



Graph 2: Comparison of our present work with the actual work done in the paper

Chapter 5

Results And Discussion

5.1 Convective Heat Transfer Performance for Al₂O₃-water based nanofluids for different Richardson numbers & volume concentration values

5.1.1 Heat Transfer Coefficient:

HTC increases with increase in volume concentration of nano particles. HTC for different Richardson's numbers ranges from 5.448133 to 108.3699. The percentage increase of HTC at 1%, 2%, 4% with respective to the HTC at 0% is calculated by:

$$\text{\% Change} = (\text{HTC at } x\% - \text{HTC at } 0\%) / \text{HTC at } 0\%$$

For Richardson number 0.1:

% change for 1% = 2.37%, for 2% = 5.50%, for 4% = 14.96

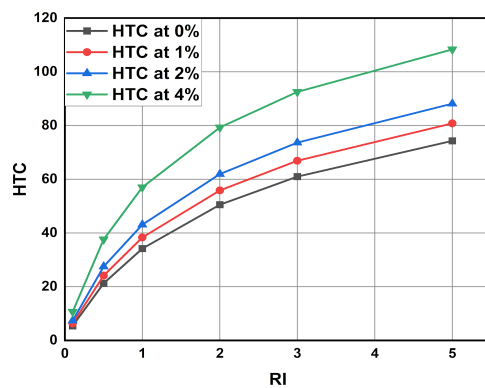
For Richardson number 2:

% change for 1% = 1.51%, for 2% = 3.59%, for 4% = 9.63

For Richardson number 5:

% change for 1% = 1.21, for 2% = 2.84%, for 4% = 7.79

As Richardson number is increasing HTC increases and after a certain Richardson number it is becoming constant.



Graph-3:

Richardson number vs average heat transfer coefficient values for different volume concentrations.

5.1.2 Nusselt Numbers:

Nusselt number increases with increase in volume concentration.

Nu value for different Richardson's number ranges from 0.09126 to 1.64696

The percentage increase of Nusselt number at 1%, 2%, 4% with respective to the Nusselt number at 0% is calculated by

$$\text{\% Change} = (\text{Nu at } x\%) - \text{Nu at } 0\% / \text{Nu at } 0\%$$

For Richardson number = 0.1:

% Change at 1% = 11.22% , 2% = 29.54% , 4% = 77.68%

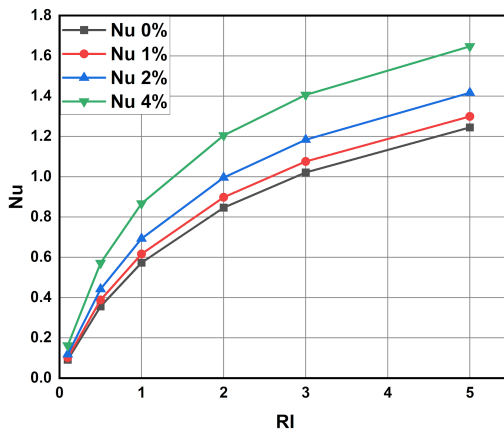
For Richardson number = 2:

% Change at 1% = 6.11% , 2% = 17.65% , 4% = 42.25%

For Richardson number = 5:

% Change at 1% = 4.39% , 2% = 13.86% , 4% = 32.25%

However the percentage of increase in Nusselt number decreases and becomes constant due to the law of diminishing returns. This Implies increasing the concentration linearly doesn't increase the Nusselt number linearly.



Graph-4: Richardson Number vs Nusselt Number values for different volume concentrations.

5.1.3 Average Shear stresses:

As the Nusselt number is increasing, average shear stress on walls is also increasing.

Average shear stress for different Richardson's number ranging from 0.0066354363 to 0.01694618. The percentage change in average shear stress compared with 0% concentration as reference are as follow

$$\% \text{ Change} = (\text{value at } x\%) - \text{value at } 0\% / \text{value at } 0\%$$

Richardson number 0.1:

% change for 1%: 15.221% for 2%: 34.783% for 4%: 102.25%

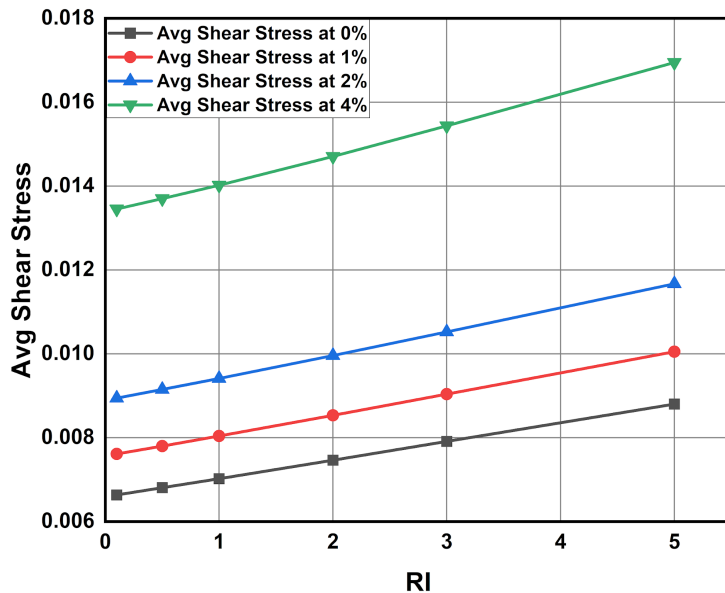
Richardson number 2:

% change for 1%: 18.346% for 2%: 32.202% for 4%: 94.158%

Richardson number 5:

% change for 1%: 25.296% for 2%: 32.576% for 4%: 92.777%

Here as concentration of nanoparticles is increasing stress are becoming 1.2 times of stress seen in pure water.

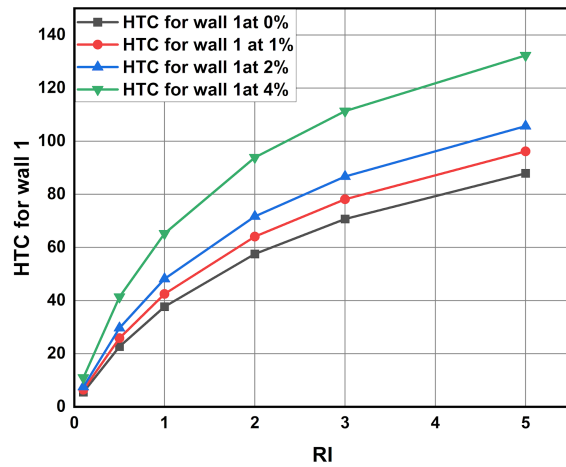


Graph-5:

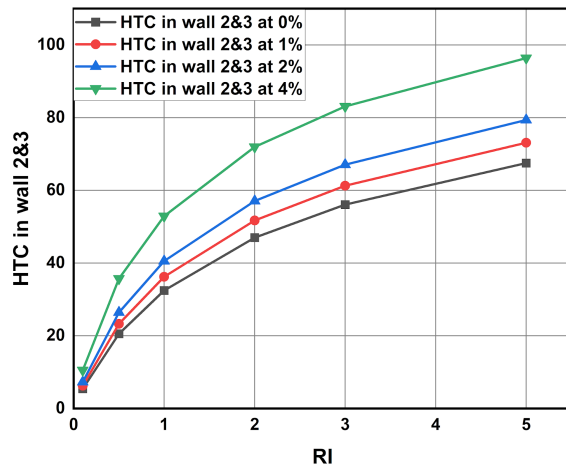
Richardson Number vs average Shear Stress values for different volume concentrations.

5.1.4 Heat Transfer Coefficient in wall-2 & wall-3 :

Here for wall 1 it has slightly higher heat transfer coefficient values compared to that wall-2 and wall-3. This is because of gravity and the weight of fluid is acting on wall-1. For wall-2 and wall-3 we are observing the same HTC values.



Graph-6: Richardson Number vs Heat transfer coefficient values in wall-1 avg for different volume concentrations.



Graph-7: Richardson Number vs Heat transfer coefficient values in wall-2 ,3 avg for different volume concentrations.

5.1.5 Pumping Powers:

Heat transfer is increasing as power required to pump the fluid into the duct is also increasing. Pumping power is increasing linearly with respect to Richardson's number.. We calculate the percentage change with 0 % as reference

$$\% \text{ Change} = (\text{value at } x\%) - (\text{value at } 0\%) / \text{value at } 0\%$$

For Richardson Number = 0.1:

$$\% \text{ change at } 1\% = 21.92\% \text{ at } 2\% = 54.176\% \text{ at } 4\% = 180.57\%$$

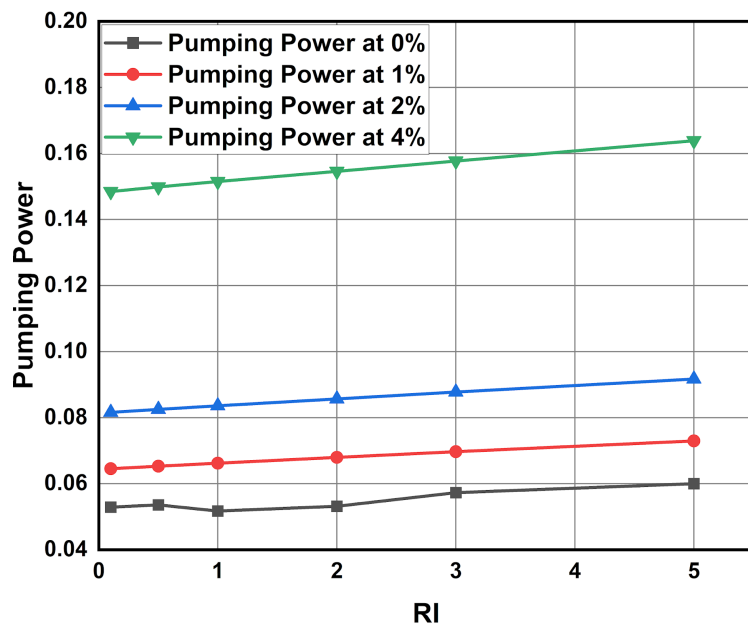
For Richardson Number = 2:

$$\% \text{ change at } 1\% = 27.87\% \text{ at } 2\% = 61.16\% \text{ at } 4\% = 192.81$$

For Richardson Number = 5:

$$\% \text{ change at } 1\% = 21.60\% \text{ at } 2\% = 52.80\% \text{ at } 4\% = 173.04\%$$

At higher concentrations and at higher Richardson's number pumping power increases



Graph-8: Richardson Number vs Pumping Power for different volume concentrations.

5.2 Convective Heat Transfer Performance for TiO_2 -water based nanofluids

5.2.1 Heat Transfer Coefficient

HTC increases with increase in volume concentration of nanoparticles. HTC for different Richardson's numbers ranges from 5.448133 to 80.0579. The percentage increase of HTC at 1%, 2%, 4% with respect to the HTC at 0% is calculated by

$$\% \text{ Change} = (\text{HTC at } x\% - \text{HTC at } 0\%) / \text{HTC at } 0\%$$

For Richard number 0.1:

$$\% \text{ change for } 1\% = 2.37\% \text{ for } 2\% = 5.61\% \text{ for } 4\% = 14.85\%$$

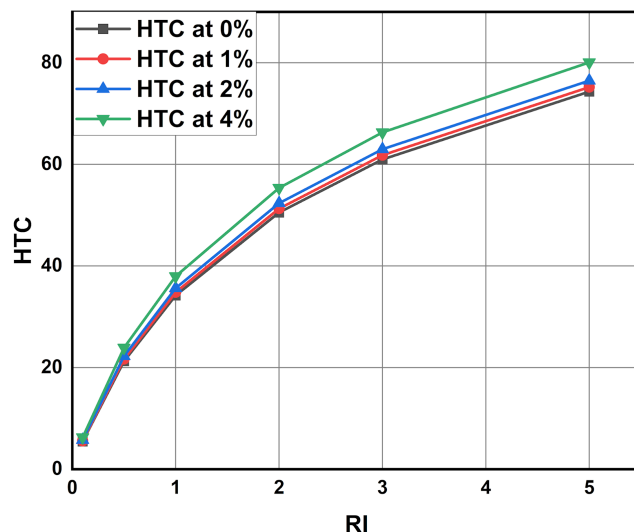
For Richard number 2:

$$\% \text{ change for } 1\% = 1.51\% \text{ for } 2\% = 3.61\% \text{ for } 4\% = 9.56$$

For Richard number 5:

$$\% \text{ change for } 1\% = 1.27\% \text{ for } 2\% = 2.9\% \text{ for } 4\% = 7.73$$

As Richardson number is increasing HTC increases and after a certain Richardson number it is becoming constant.



Graph-9: Richardson number vs average heat transfer coefficient values for different volume concentrations.

5.2.2 Nusselt Numbers:

Nusselt number increases with increase in volume concentration. Nu value for different Richardson's numbers ranges from 0.09126 to 1.64696 . The percentage increase of Nusselt number at 1%,2%,4% with respective to the Nusselt number at 0% is calculated by

$$\% \text{ Change} = (\text{Nu at } x\%) - \text{Nu at } 0\% / \text{Nu at } 0\%$$

For Richardson number = 0.1:

$$\% \text{ Change at } 1\% = 2.119\% , 2\% = 5.205\% , 4\% = 14.149\%$$

For Richardson number = 2:

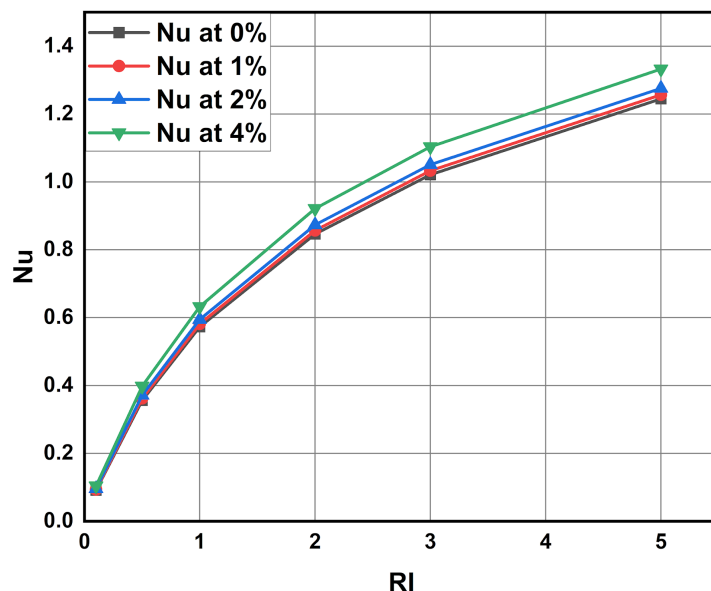
$$\% \text{ Change at } 1\% = 1.2639\% , 2\% = 3.21\% , 4\% = 8.827\%$$

For Richardson number = 5:

$$\% \text{ Change at } 1\% = 0.9585\% , 2\% = 2.511\% , 4\% = 7.0794\%$$

However the percentage of increase in Nusselt number decreases and becomes constant due to the law of diminishing returns.

This Implies increasing the concentration linearly doesn't increase the Nusselt number linearly.



Graph-10: Richardson Number vs Nusselt Number values for different volume concentrations.

5.2.3 Average Shear stresses:

As Nusselt number is increasing, average shear stress on walls is also increasing. Average shear stress for different Richardson's numbers ranges from 0.0066354363 to 0.01694618.

The percentage increase of Average shear stress at 1%, 2%, 4% with respective to the value at 0% is calculated by

$$\% \text{ Change} = (\text{value at } x\% - \text{value at } 0\%) / \text{value at } 0\%$$

Richardson number 0.1:

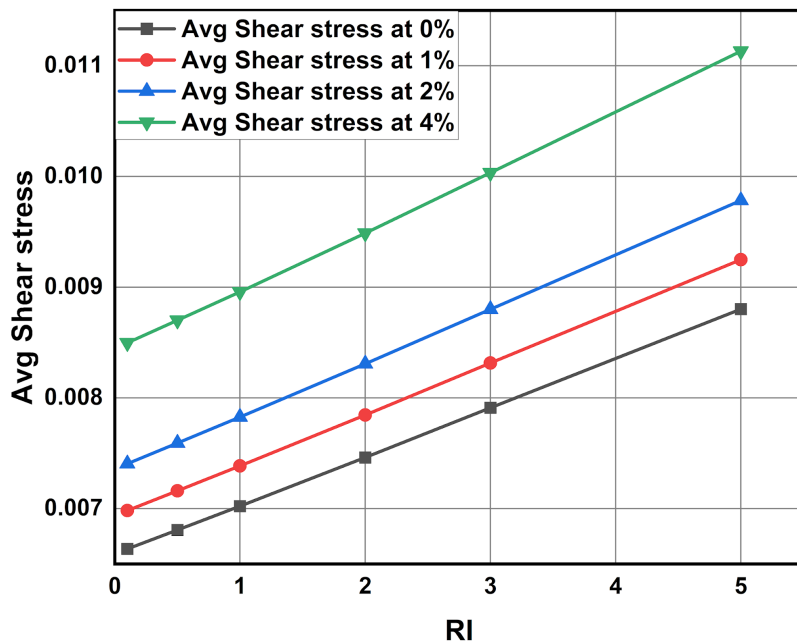
% change for 1%: 5.2301% for 2%: 11.604% for 4%: 28.059

Richardson number 2:

% change for 1%: 5.139% for 2%: 11.336% for 4%: 27.148%

Richardson number 5:

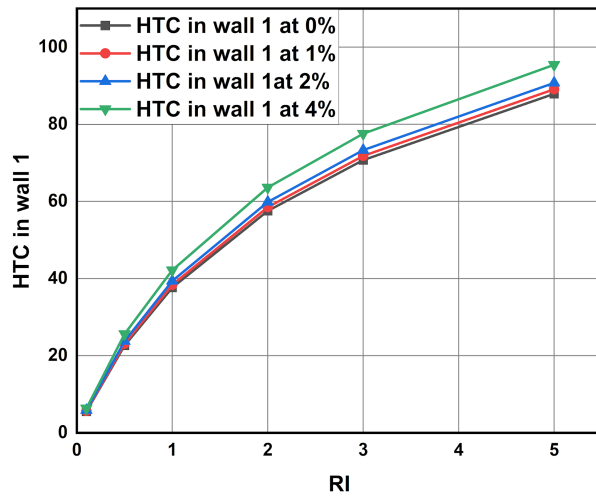
% change for 1%: 5.0911% for 2%: 11.16% for 4%: 26.482%



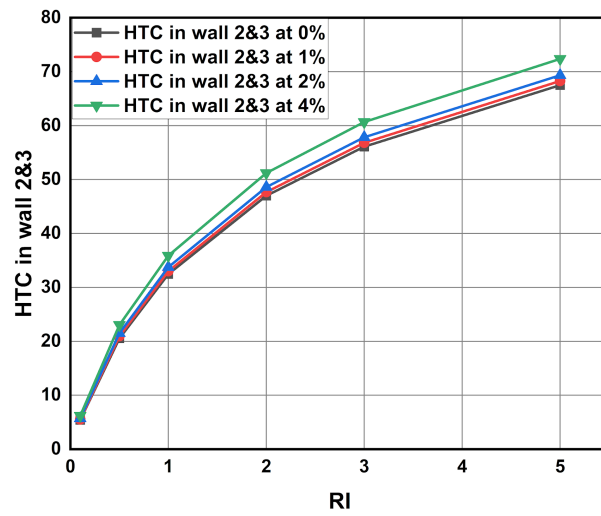
Graph-11: Richardson Number vs average Shear Stress values for different volume concentrations.

5.2.4 Heat Transfer Coefficient in wall-1 and wall 2&3 Avg

Here for wall 1 it has slightly higher heat transfer coefficient values compared to that wall-2 and wall-3. This is because of gravity and the weight of fluid is acting on wall-1. For wall-2 and wall-3 we are observing the same HTC values.



Graph-12: Richardson Number vs Heat transfer coefficient values in wall-1 for different volume concentrations.



Graph-13: Richardson Number vs Heat transfer coefficient values in wall-1 for different volume concentrations.

5.2.5 Pumping Power:

Here as Heat transfer is increasing power required to pump the fluid into duct is also increasing. Pumping power is increasing linearly with respect to Richardson's number.

We calculate the percentage change with 0 % as reference

$$\% \text{ Change} = (\text{value at } x\%) - (\text{value at } 0\%) / \text{value at } 0\%$$

For Richardson Number = 0.1:

$$\% \text{ change at } 1\% = 22.05\% \text{ at } 2\% = 54.31\% \text{ at } 4\% = 180.32$$

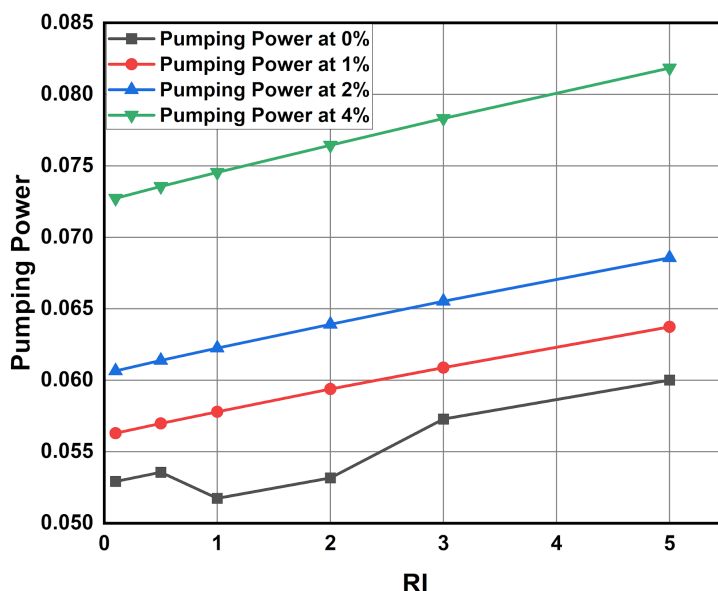
For Richardson Number = 2:

$$\% \text{ change at } 1\% = 27.85\% \text{ at } 2\% = 61.23\% \text{ at } 4\% = 191.95\%$$

For Richardson Number = 5:

$$\% \text{ change at } 1\% = 21.55\% \text{ at } 2\% = 52.77\% \text{ at } 4\% = 173.03\%$$

At higher concentrations and at higher Richardson's number pumping power required is becoming more.



Graph-14: Richardson Number vs Pumping Power for different volume concentrations.

5.3 Convective Heat Transfer Performance for SiO_2 - water based nanofluids

5.3.1 Heat Transfer Coefficient:

HTC increases with increase in volume concentration of nanoparticles. HTC for different Richardson's number ranges from 6.239 to 79.270. The percentage increase of HTC at 1%, 2%, 4% with respective to the HTC at 0% is calculated by:

$$\% \text{ Change} = (\text{HTC at } x\%) - \text{HTC at } 0\% / \text{HTC at } 0\%$$

For Richard number 0.1:

$$\% \text{ change for } 1\% = 3.484 \% \text{ for } 2\% = 6.96\% \text{ for } 4\% = 14.53\%$$

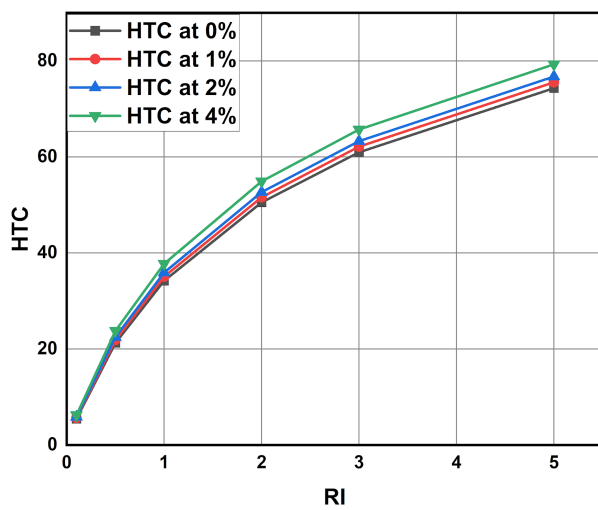
For Richard number 2:

$$\% \text{ change for } 1\% = 2.1295\% \text{ for } 2\% = 4.217\% \text{ for } 4\% = 8.66\%$$

For Richard number 5:

$$\% \text{ change for } 1\% = 1.6531 \% \text{ for } 2\% = 3.27\% \text{ for } 4\% = 6.67\%$$

As Richardson number is increasing HTC increases and after a certain Richardson number it is becoming constant.



Graph-15: Richardson number vs average heat transfer coefficient values for different volume concentrations.

5.3.2 Nusselt Numbers:

Nusselt number increases with increase in concentration. Nu value for different Richardson's number ranges from 0.102 to 1.307. The percentage increase of Nusselt number at 1%, 2%, 4% with respective to the Nusselt number at 0% is calculated by

$$\% \text{ Change} = (\text{Nu at } x\%) - \text{Nu at } 0\% / \text{Nu at } 0\%$$

For Richardson number = 0.1:

$$\% \text{ Change at } 1\% = 2.84\% , 2\% = 5.918\% , 4\% = 12.77\%$$

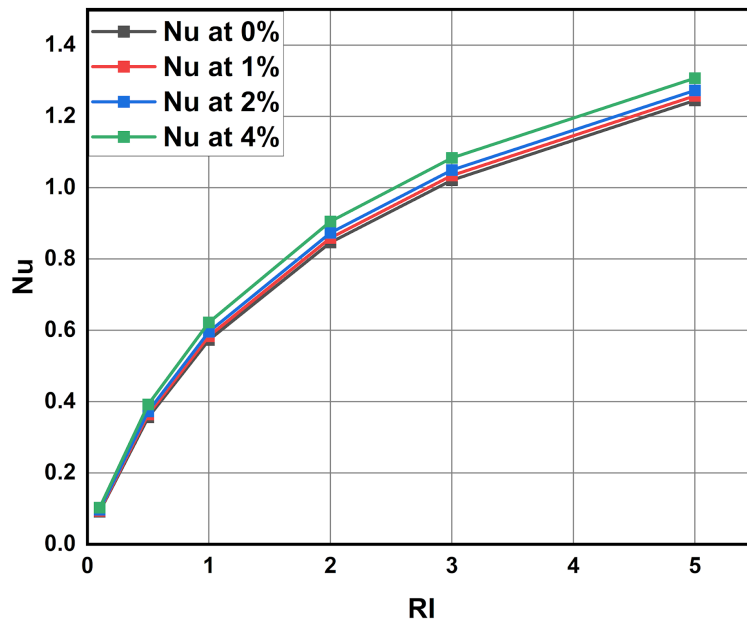
For Richardson number = 2:

$$\% \text{ Change at } 1\% = 1.4976\% , 2\% = 3.2019\% , 4\% = 6.9961\%$$

For Richardson number = 5:

$$\% \text{ Change at } 1\% = 1.1241\% , 2\% = 2.2645\% , 4\% = 5.0454\%$$

However the percentage of increase in Nusselt number decreases and becomes constant due to the law of diminishing returns. This implies increasing the concentration linearly doesn't increase the Nusselt number linearly



Graph-16: Richardson Number vs Nusselt Number values for different volume concentrations.

5.3.3 Average Shear stresses:

As the Nusselt number is increasing, average shear stress on walls is also increasing. Average shear stress for different richardson's number ranges from 0.0066354363 to 0.01022

The percentage change in average shear stress compared with 0% concentration as reference are as follows

$$\text{\% Change} = (\text{value at } x\%) - \text{value at } 0\% / \text{value at } 0\%$$

For Richard number 0.1:

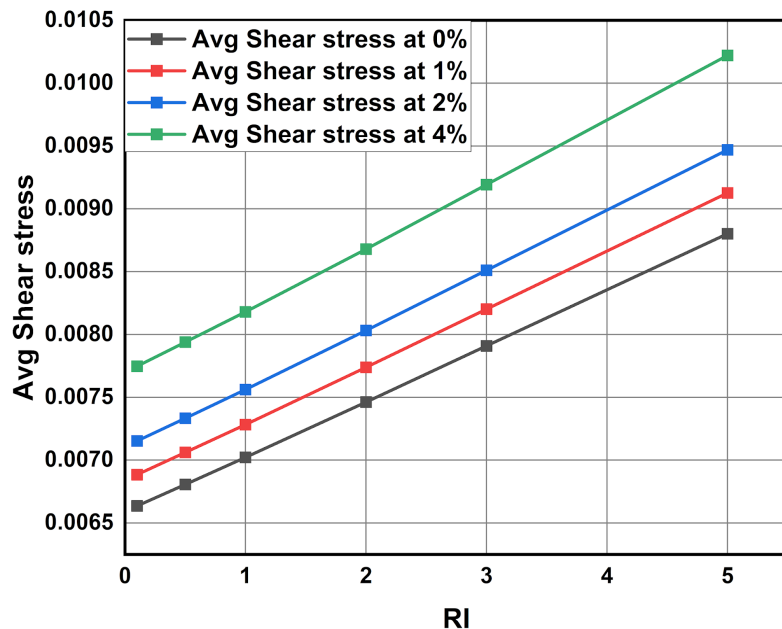
% change for 1% = 3.7535% for 2% = 7.794% for 4% = 16.72

For Richard number 2:

% change for 1% = 3.6982% for 2% = 3.59% for 4%: 16.312%

For Richard number 5:

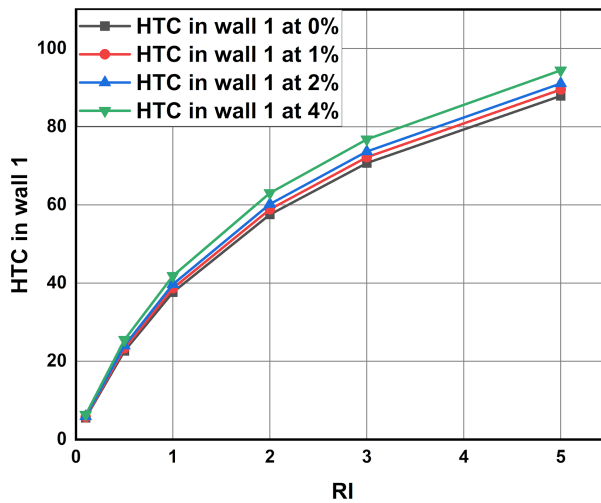
% change for 1% = 3.6979 for 2% = 7.5857% for 4%: 16.182%



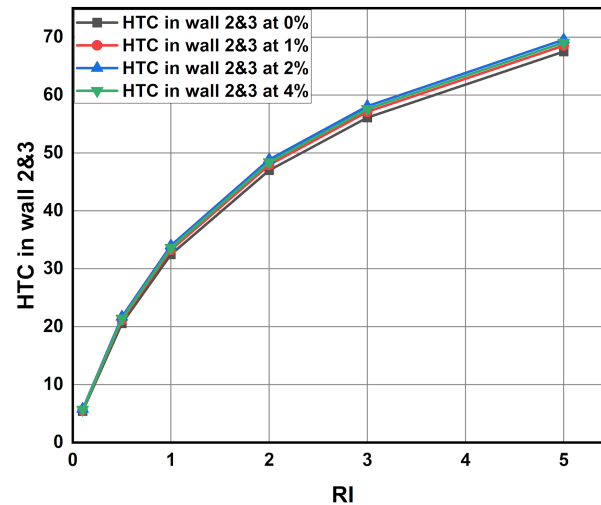
Graph-17: Richardson Number vs average Shear Stress values for different volume concentrations.

5.3.4 Heat Transfer Coefficient in wall-1 and wall-2&3:

Here for wall 1 it has slightly higher heat transfer coefficient values compared to that wall-2 and wall-3. This is because of gravity and the weight of fluid is acting on wall-1. For wall-2 and wall-3 we are observing the same HTC values.



Graph-18: Richardson Number vs Heat transfer coefficient values in wall-1 for different volume concentrations.



Graph-19: Richardson Number vs Heat transfer coefficient values in wall-1 for different volume concentrations.

5.3.5 Pumping Power

Heat transfer is increasing power required to pump the fluid into the duct. Pumping power is increasing linearly with respect to Richardson's number. The range of pumping power is 0.0592 and 0.0852

The percentage change with 0% concentration as reference are as follow

$$\% \text{ Change} = (\text{value at } x\%) - (\text{value at } 0\%) / \text{value at } 0\%$$

For Richardson Number = 0.1:

$$\% \text{ change at } 1\% = 3.87\% \text{ at } 2\% = 11\% \text{ at } 4\% = 42\%$$

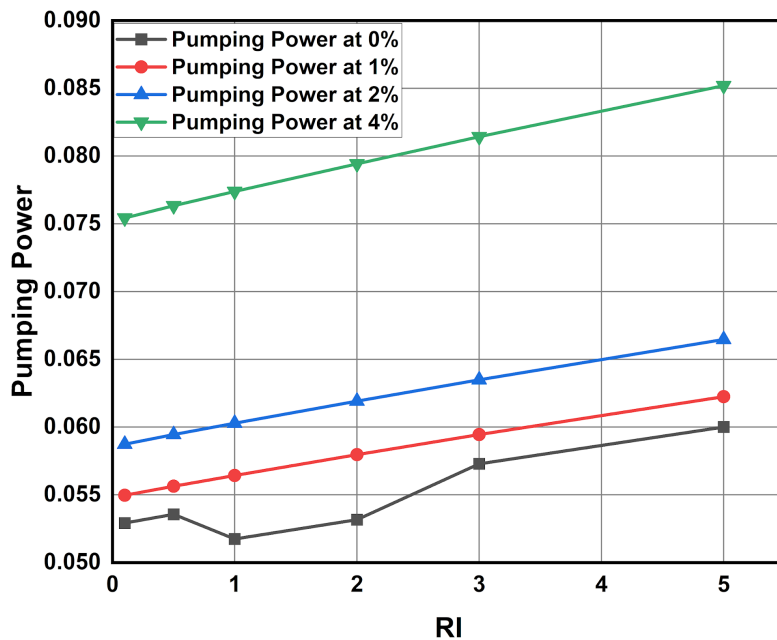
For Richardson Number = 2:

$$\% \text{ change at } 1\% = 9.025\% \text{ at } 2\% = 16.44\% \text{ at } 4\% = 49.392\%$$

For Richardson Number = 5:

$$\% \text{ change at } 1\% = 3.728\% \text{ at } 2\% = 10.76\% \text{ at } 4\% = 41.984\%$$

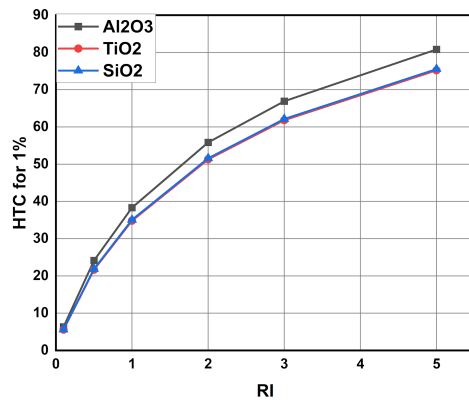
At higher concentrations and at higher Richardson's number pumping power required is becoming more.



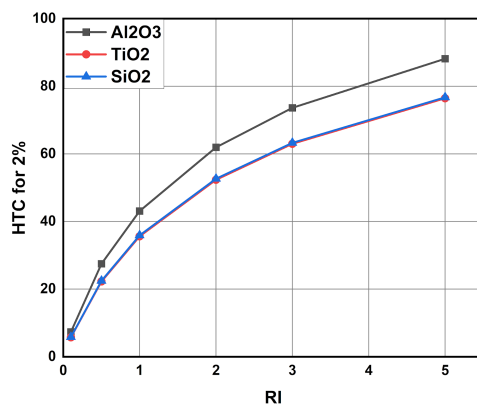
Graph-20: Richardson Number vs Pumping Power for different volume concentrations.

5.4 Comparing Convective heat transfer performance between nanofluids using analytical data

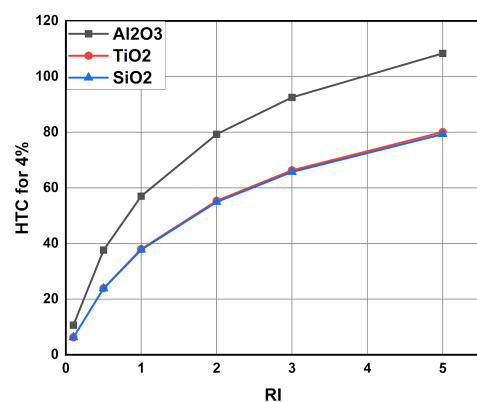
5.4.1 Comparing HTC



Graph-21: Heat transfer coefficient for various nanofluids at 1% volume concentration



Graph-22: Heat transfer coefficient for various nanofluids at 2% volume concentration

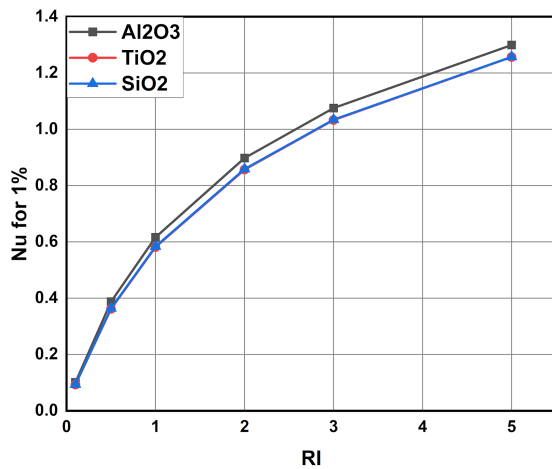


Graph-23: Heat transfer coefficient for various nanofluids at 4% volume concentration

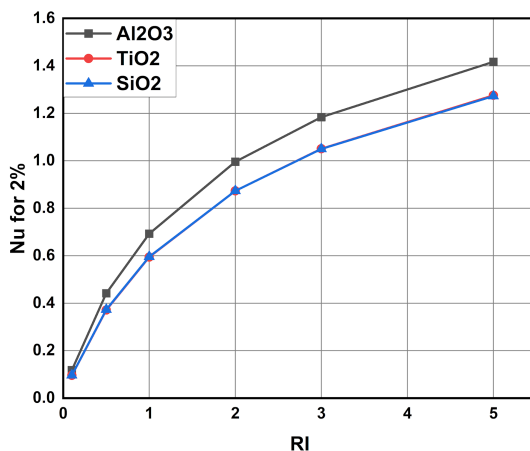
Here Aluminium oxide nanofluid has greater heat transfer coefficient than silicon oxide or titanium oxide of around 108.36 vs 79.270 Water based Silicon oxide and Titanium oxide nanofluids has almost very same thermo-physical properties difference between those values is very less Nearly around 79.270

As volume concentration increases, the gap between Aluminium-oxide nanofluids and silicon oxide nanofluids increases, showing that as volume concentration is increasing, Aluminium oxide is showing greater sensitivity and providing higher heat transfer coefficient.

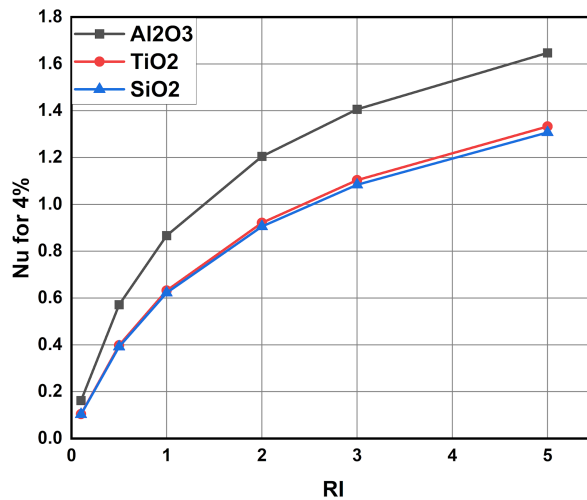
5.4.2 Comparing Nusselt Number



Graph-24: Nusselt Number for various nanofluids at 1% volume concentration



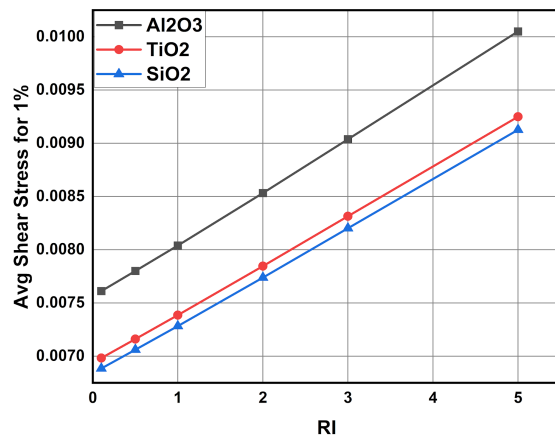
Graph-25: Nusselt Number for various nanofluids at 2% volume concentration



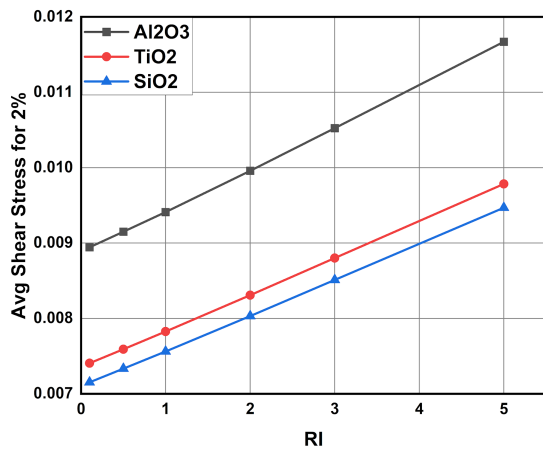
Graph-26: Nusselt Number for various nanofluids at 4% volume concentration

Here water + aluminium oxide based has higher Nusselt number among the other two nanofluids. For Aluminium oxide nanofluid at 1% volume concentration , Nusselt number is varying from 0 to 1.4, at 2% volume concentration Nusselt number is varying from 0 to 1.6 and at 4% volume concentration Nusselt number is varying from 0 to 1.8. Whereas for titanium and silicon oxide nanofluids it is varying from 0 to 1.4 at all concentrations and values for both nanofluids are very close to each other. Comparatively Silicon oxide-water based nanofluid has lower Nusselt number.

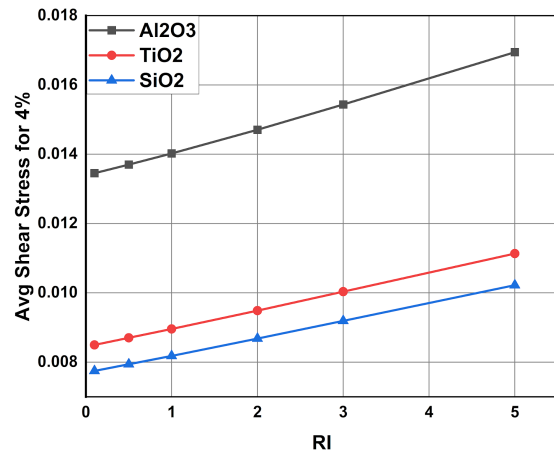
5.4.3 Comparing Average Shear Stress



Graph-27: Average shear stress for various nanofluids at 2% volume concentration



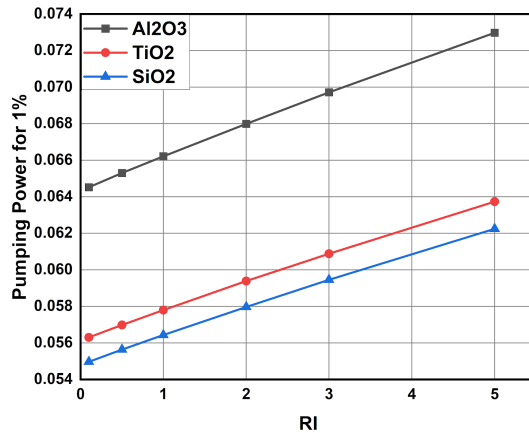
Graph-28: Average shear stress for various nanofluids at 1% volume concentration



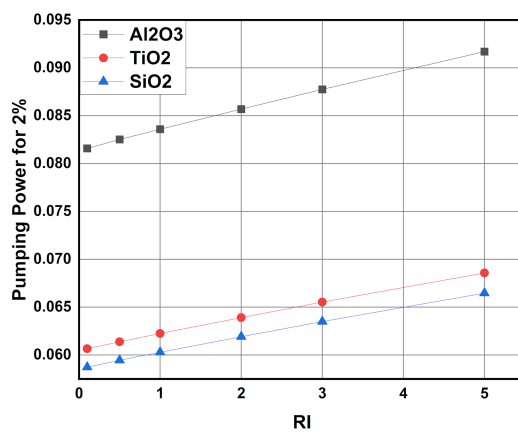
Graph-29: Average shear stress for various nanofluids at 4% volume concentration

Along with heat transfer coefficient Aluminum oxide nanofluid also has higher shear stress around the walls of the duct (0.0169) As concentration increases gap between silicon oxide and titanium oxide increases and at 4% volume concentration titanium oxide has higher shear stress which is undesirable.(0.0113 vs 0.0102) Silicon oxide nanofluid is giving us very less shear stress. 0.0102

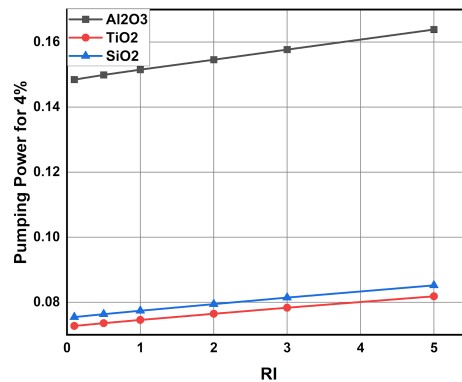
5.4.4 Comparing Results between Pumping Power:



Graph-30: Pumping power for various nanofluids at 1% volume concentration



Graph-31: Pumping power for various nanofluids at 2% volume concentration



Graph-32: Pumping power for various nanofluids at 4% volume concentration

Pumping power required for Water based Aluminium oxide nanofluids is (0.1685 at 4 % concentration) more compared to silicon oxide and titanium oxide nanofluids. Pumping power required for Titanium oxide nanofluid is more than that required for silicon oxide nanofluid at lower volume concentrations. (0.07543 vs 0.07274).As concentration increases Silicon oxide having pumping power of than that of Titanium oxide nanofluid (0.0818 vs 0.0852)

5.5 Observing Convective heat transfer performance between Nanofluids using streamline contours

5.5.1 Contours of Aluminium Oxide NanoFluid:

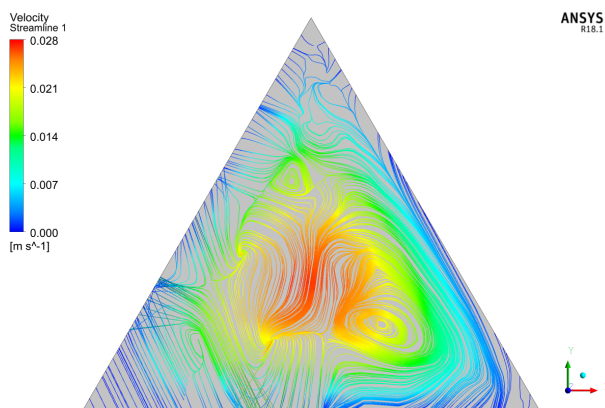


Figure-3: Velocity Streamline at midpoint(1000mm) at 4% volume concentration and Richardson number=0.1

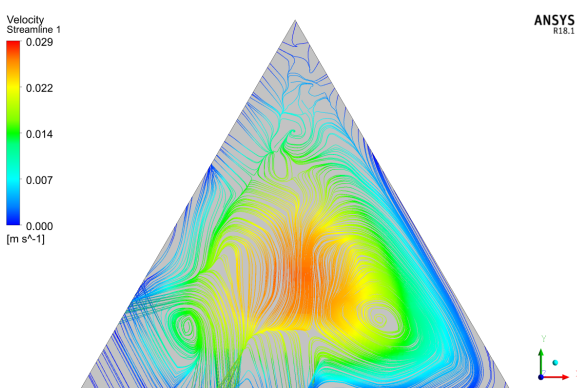


Figure-4: Velocity Streamline at midpoint(1000mm) at 4% volume concentration and Richardson number=0.5

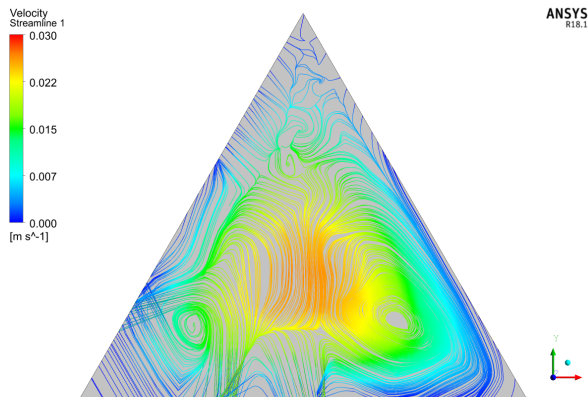


Figure-5: Velocity Streamline at midpoint(1000mm) at 4% volume concentration and Richardson number=1

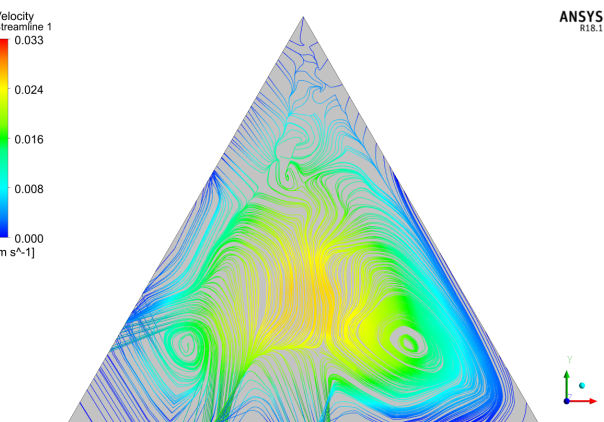


Figure-6: Velocity Streamline at midpoint(1000mm) at 4% volume concentration and Richardson number=2

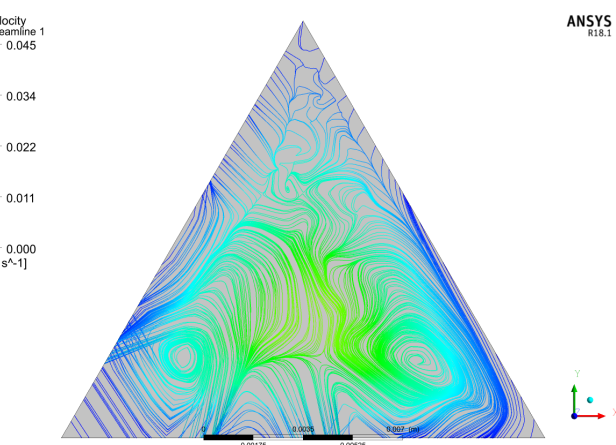


Figure-7: Velocity Streamline at midpoint(1000mm) at 4% volume concentration and Richardson number=5

Inference:

5.5.2 Contours of Titanium Oxide NanoFluid:

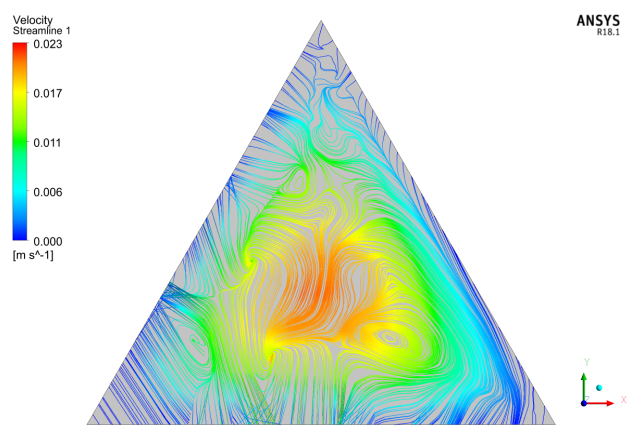


Figure-8: Velocity Streamline at midpoint(1000mm) at 0% volume concentration and Richardson number=0.1

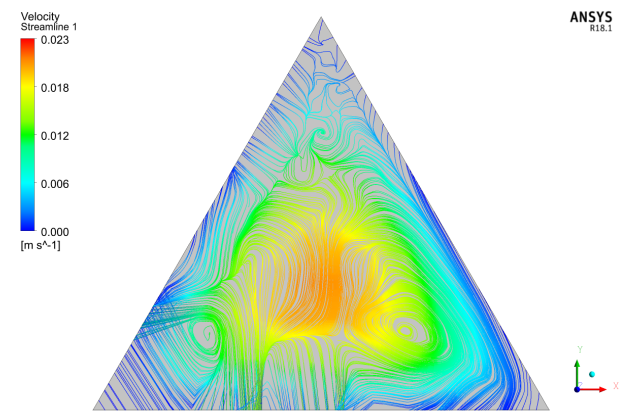


Figure-9: Velocity Streamline at midpoint(1000mm) at 0% volume concentration and Richardson number=0.5

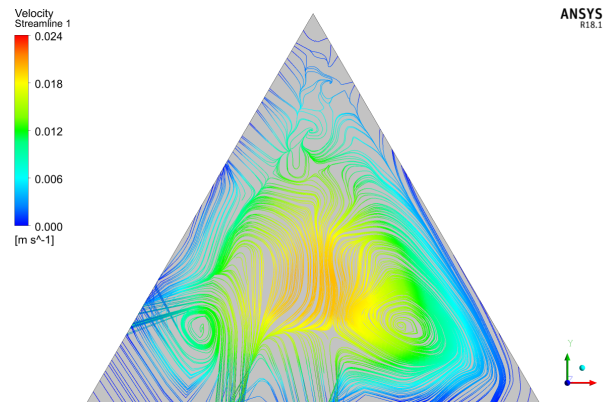


Figure-10: Velocity Streamline at midpoint(1000mm) at 0% volume concentration and Richardson number=1

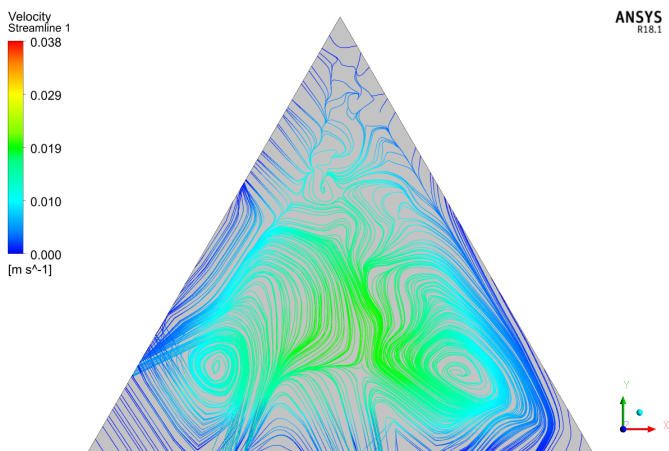


Figure-11: Velocity Streamline at midpoint(1000mm) at 0% volume concentration and Richardson number=5

Inference:

5.5.3 Contours of Silicon Oxide NanoFluids:

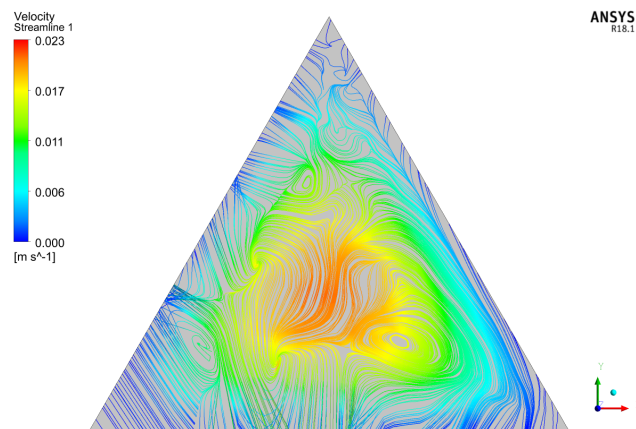


Figure-12: Velocity Streamline at midpoint(1000mm) at 0% volume concentration and Richardson number=0.1

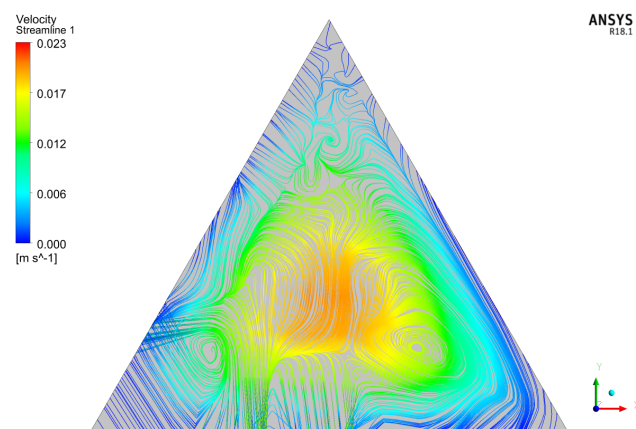


Figure-13: Velocity Streamline at midpoint(1000mm) at 0% volume concentration and Richardson number=0.5

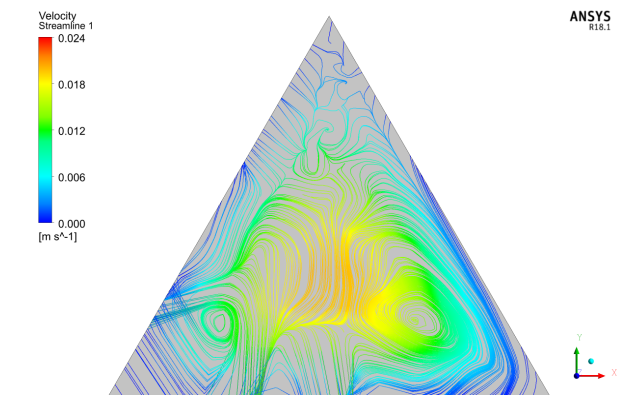


Figure-14: Velocity Streamline at midpoint(1000mm) at 0% volume concentration and Richardson number=1

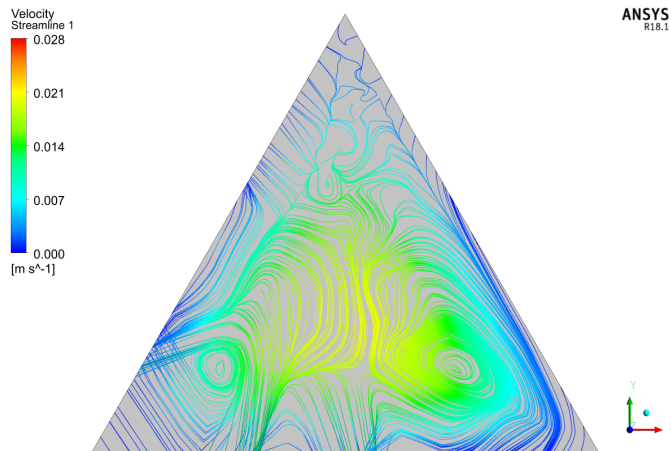


Figure-15: Velocity Streamline at midpoint(1000mm) at 0% volume concentration and Richardson number=2

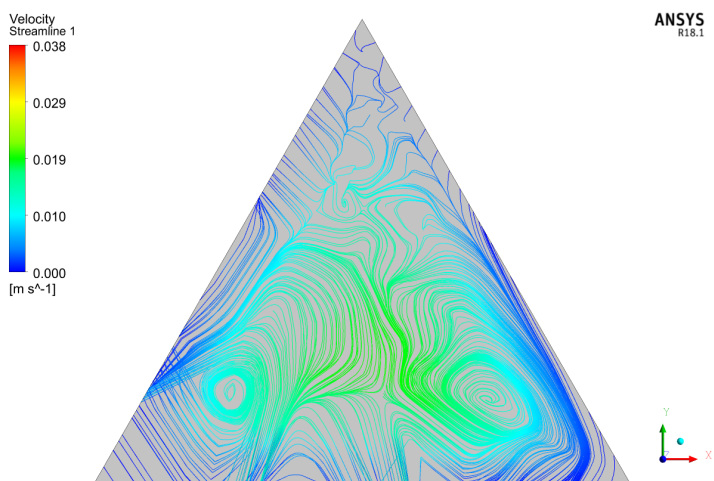


Figure-16: Velocity Streamline at midpoint(1000mm) at 0% volume concentration and Richardson number=5

Inference:

Conclusions:

1. Water based Aluminium oxide nanofluid has higher heat transfer properties, it has greater Nusselt numbers and heat transfer coefficients. Also as Volume concentrations increase, properties are also getting improved with greater heat transfer.
2. The only disadvantage of using Aluminium oxide-water based nanofluid is, it requires higher pumping power and also greater shear stresses are generated along the walls.
3. Titanium oxide-water based nanofluid has better heat transfer capacity rather than the Silicon oxide-water based nanofluid.
4. But silicon oxide-water based nanofluid requires lesser pumping power and having lesser shear stresses at lower concentrations.

Chapter 6

Future Plan

- We would like to increase the accuracy of the results.
- We would like to do the analysis under forced convection with various fluids flowing over it, at present we used natural convection.
- We consider these models as a stepping stone and modify them for increased heat dissipation.

Flow in Ducts

Nomenclature:

A: Cross-section area (m^2)

H: Duct height (m)

c_p: Specific heat (J/kgK)

l: Duct edge length (m)

d: Duct diameter (m)

L: Total duct length (m)

f: Friction factor

Nu: Nusselt number

g: Gravitational acceleration (m/s^2)

P: Pressure (Pa)

Gr: Grashof number

Pe: Peclet number

h: Heat transfer coefficient ($\text{W/m}^2\text{K}$)

PP: Pumping power (W)

Pr: Prandtl number(ν/a)

ρ : Density (kg/m^3)

q : Heat flux (W/m^2)

τ : Wall shear stress (kg/m)

Re: Reynolds number

ν : Kinematic viscosity (m^2/s)

Ri: Richardson number

π : Nanoparticle volumetric concentration.

T: Temperature (K)

Subscripts:

u, v, w : Velocity component (m/s)

avg: Average

V: Average velocity (m/s)

b_f : Base fluid

v: Volume flow rate (m^3/s)

f: Fluid

x, y, z : Spatial coordinates (m).

h: Hydraulic

Greek Symbols:

m: Mass

α : Thermal diffusivity (m^2/s)

n_f : Nanofluid

β : Volumetric expansion coefficient ($1/\text{K}$)

p: Solid particle

λ : Thermal conductivity ($\text{W}/\text{m K}$)

w: Wal

μ : Dynamic viscosity (Pa s)

References

- [1] Aggarwala, B. D., & Gangal, M. K. (1975). Laminar flow development in triangular ducts. *Transactions of the Canadian Society for Mechanical Engineering*, 3(4), 231–233. <https://doi.org/10.1139/tcsme-1975-0031>

- [2] Buongiorno, J., Venerus, D. C., Prabhat, N., McKrell, T., Townsend, J., Christianson, R., Tolmachev, Y. V., Keblinski, P., Hu, L.-W., Alvarado, J. L., Bang, I. C., Bishnoi, S. W., Bonetti, M., Botz, F., Cecere, A., Chang, Y., Chen, G., Chen, H., Chung, S. J., ... Zhou, S.-Q. (2009). A benchmark study on the thermal conductivity of

nanofluids. *Journal of Applied Physics*, 106(9), 094312.
<https://doi.org/10.1063/1.3245330>

[3] Ferrouillat, S., Bontemps, A., Ribeiro, J.-P., Gruss, J.-A., & Soriano, O. (2011). Hydraulic and heat transfer study of SiO₂/water nanofluids in horizontal tubes with imposed wall temperature boundary conditions. *International Journal of Heat and Fluid Flow*, 32(2), 424–439. <https://doi.org/10.1016/j.ijheatfluidflow.2011.01.003>

[4] Hanks, R. W., & Cope, R. C. (1970). Laminar-turbulent transitional flow phenomena in isosceles triangular cross-section ducts. *AICHE Journal. American Institute of Chemical Engineers*, 16(4), 528–535. <https://doi.org/10.1002/aic.690160405>

[5] Mohammed, H. A., Om, N. I., Shuaib, N. H., Hussein, A. K., & Saidur, R. (2011). The application of nanofluids on three dimensional mixed convection heat transfer in equilateral triangular duct. *Heat and Technology*, 29(2), 3–12.
<https://eprints.um.edu.my/6691/>

[6] Montgomery, S. R., & Wibulsvas, P. (2019). Laminar flow heat-transfer in ducts of rectangular cross-section. *Proceeding of International Heat Transfer Conference 3.*

[7] Xuan, Y., & Li, Q. (2000). Heat transfer enhancement of nanofluids. *International Journal of Heat and Fluid Flow*, 21(1), 58–64.
[https://doi.org/10.1016/s0142-727x\(99\)00067-3](https://doi.org/10.1016/s0142-727x(99)00067-3)

[8] Yilmaz, T., & Cihan, E. (1993). General equation for heat transfer for laminar flow in ducts of arbitrary cross-sections. *International Journal of Heat and Mass Transfer*, 36(13), 3265–3270. [https://doi.org/10.1016/0017-9310\(93\)9000](https://doi.org/10.1016/0017-9310(93)9000)

[9] Zhou, S.-Q., & Ni, R. (2008). Measurement of the specific heat capacity of water-based Al₂O₃ nanofluid. *Applied Physics Letters*, 92(9), 093123.
<https://doi.org/10.1063/1.2890431>

[10] Talukdar P., Shah M., “Analysis of laminar mixed convective heat transfer in horizontal triangular ducts,” *Numerical Heat Transfer Part A: Applications*, vol. 54, no. 12, pp. 1148–1168, 2008.

[11] Lawal A., “Mixed convection heat transfer to power law fluids in arbitrary cross-sectional ducts,” *Journal of Heat Transfer*, vol. 111, no. 2, pp. 399–406, 1989.

- [12] Schneider G. E., LeDain B. L., “Fully developed laminar heat transfer in triangular passages,” *Journal of energy*, vol. 5, no. 1, pp. 15–21, 1981.
- [13] Hanks R. W., Cope R. C., “Laminar-Turbulent Transitional Flow Phenomena in Isosceles Triangular Cross-section Ducts,” *AICHE Journal*, vol. 16, no. 4, pp. 528–535, 1970.
- [14] Altemani C. A. C., Sparrow E. M., “Turbulent heat transfer and fluid flow in an unsymmetrically heated triangular duct,” *Journal of Heat Transfer*, vol. 102, no. 4, pp. 590–597, 1980.
- [15] Leung C. W., Wong T. T., and Kang H. J., “Forced convection of turbulent flow in triangular ducts with different angles and surface roughnesses,” *Heat and Mass Transfer*, vol. 34, no. 1, pp. 63–68, 1998. <https://www.sciencedirect.com/science/article/abs/pii/S0142727X11000117>
- [16] Sharabi M., Ambrosini W., He S., and Jackson J. D., “Prediction of turbulent convective heat transfer to a fluid at supercritical pressure in square and triangular channels,” *Annals of Nuclear Energy*, vol. 35, no. 6, pp. 993–1005, 2008.. .
- [17] Chaves C. L., Quaresma J. N. N., Mac`do N., Mac  do E. N., Pereira L. M., and Lima J. A., “Forced convection heat transfer to power-law non-Newtonian fluids inside triangular ducts,” *Heat Transfer Engineering*, vol. 25, no. 7, pp. 23–33, 2004.
- [18] Manca O., Nardini S., Ricci D., and Tamburrino S., “Numerical investigation on mixed convection in triangular cross-section ducts with nanofluids,” *Advances in Mechanical Engineering*, vol. 2012, Article ID 139370, 13 pages, 2012.
- [19] Rehme K., “Simple method of predicting friction factors of turbulent flow in non-circular channels,” *International Journal of Heat and Mass Transfer*, vol. 16, no. 5, pp. 933–950, 1973.
- [20] Lai Y. G., “An unstructured grid method for a pressure-based flow and heat transfer solver,” *Numerical Heat Transfer, Part B: Fundamentals*, vol. 32, no. 3, pp. 267–281, 1997.
- [21] Chen S., Chan T. L., Leung C. W., and Yu B., “Numerical prediction of laminar forced convection in triangular ducts with unstructured triangular grid

method," Numerical Heat Transfer Part A: Applications, vol. 38, no. 2, pp. 209–224, 2000.

[22] Shah R. K., London A. L., Laminar Flow Forced Convection in Ducts, Academic Press, New York, NY, USA, 1978.